

# On the dynamics and control of complex phenomena in parametrically driven chains of pendulums

Laura Marcheggiani<sup>1</sup>, Stefano Lenci<sup>1</sup>, Ricardo Chacon<sup>2</sup>

<sup>1</sup>*Department of Architecture, Buildings and Structures, Polytechnic University of Marche, Ancona, Italy*  
*E-mail: l.marcheggiani@univpm.it, lenci@univpm.it*

<sup>2</sup>*Department of Applied Physics, Faculty of Industrial Engineering, University of Extremadura, Badajoz, Spain*  
*E-mail: rchacon@unex.es*

*Keywords:* Synchronization phenomena, coupled pendulums chains, control.

**SUMMARY.** A model of a multidimensional system, consisting of a chain of nonlinearly coupled chaotic pendula subjected to a chaos-inducing harmonic parametric excitation, is introduced. The nonlinear dynamics of the chain is analyzed with attention to the synchronization phenomena. The control of chaos (suppression and enhancement) through the introduction of a second periodic excitation is investigated, by a numerical approach (Lyapunov exponents), firstly with reference to the simple case of a single pendulum; then the effectiveness of the method is studied on the chain, by applying the localized control on a minimal number of pendula.

## 1 INTRODUCTION

A simple parametric pendulum is a classical nonlinear dynamic system which has been of scientific interest for a considerable amount of time. It has been found that this system can generate various types of motion, from simple periodic oscillation to complex chaos [1]. The system motion depends on the initial condition, the excitation frequency and amplitude, and on the parameters of the pendulum, such as the length of the pendulum rod.

Complex multidimensional systems consisting of chains of identical coupled chaotic pendula present a non-trivial dynamics which has attracted, in the last decades, the attention of the scientific community and which is still under study; in particular there is a growing interest in understanding and controlling the synchronization and desynchronization phenomena in networks of coupled chaotic oscillators [2, 3]; this topic is currently under investigation in physics, biology and technology for the wide area of practical applications (laser systems [4], fluid mixing [5], secure information processing [6], plasma systems [7], neuronal stimuli transmissions [8, 9], and pedestrians-structure interaction [10, 11], to cite just a few) as well as of fundamental theoretical open issues. Moreover, strictly related with synchronization-desynchronization transitions, in the context of chaotic arrays, there is the ubiquitous problem of controlling chaos, which is reflected in an abundant literature [12-14], including experimental control [15, 16].

Since the first proposals for control and synchronization of chaos, many other approaches have been suggested for chaos control [12, 13], while the concept of chaotic synchronization has been extended to those of phase synchronization and lag synchronization and the transition between different types of synchronization processes has been studied [2, 17].

Both in control and in synchronization of chaos, a chaotic dynamics is conveniently disturbed by means of an external perturbation (usually small as compared with the unperturbed dynamics),

in order to force the appearance of a goal behaviour compatible with the natural evolution of the system. Among the different control methods which have been proposed in recent years, the so-called open loop small perturbations [18, 19] has been shown to be quite reliable and readily experimentally applicable [16]. It is especially advantageous in situations where no possibility to measure the system's variables exists, such as ultrafast processes at the molecular or atomic level. In particular, a theoretical approach to chaos control in dissipative non-autonomous systems capable of being proved by Melnikov's analysis (MA) by adding periodic chaos-controlling (CC) excitations has been developed since the beginning of 1990's [20]. This MA-based approach has been shown to be effective to tame chaos in coupled arrays of damped, periodically forced, nonlinear oscillators [12]. Two main cases with respect to the two types of involved periodic excitations (one chaos-inducing (CI) and the other CC) have been considered till now in the literature: (i) two external excitations (forcings), and (ii) one external excitation and the other parametric. The physically relevant case where both excitations are parametric has not been however studied in detail yet, to the best of our knowledge, in spite of its great theoretical and technological interest. In this context we begin the study of such a control scenario, considering the case of the main resonance between the two involved parametric excitations; our approach is numerical, as we consider excitation amplitudes which do not fit reasonably the MA smallness requirements [20, 21].

In this present work, our model of chain of dissipative Kapitza pendula is introduced and its dynamics is investigated with attention to synchronization phenomena (Section 2). A control scenario based on the addition of a chaos-controlling (CC) periodic parametric excitation is numerically analyzed, firstly for the paradigmatic example of a single dissipative Kapitza pendulum and then for the generic chain of  $N$  pendula (Section 3). The effectiveness of the control method under localized application of the CC excitations on a minimal number of pendula in the chain is studied for the case of the main resonance between the two different kinds of involved parametric excitations (one chaos-inducing and the others chaos-controlling). Finally some concluding remarks are drawn in Section 4.

## 2 THE MODEL

We consider a complex multidimensional system consisting of a chain of  $N$  damped, parametrically and periodically driven pendula which are nonlinearly coupled between them; the pendula are connected at the level of their points of support with a rigid rod and they are coupled at the level of their masses with springs. The parametric excitation is vertical and sinusoidal, it is applied to the common support of the chain and therefore it is the same for all the pendula.

The mathematical model of our  $N$ -dimensional dynamical system is derived by writing the exact equations of motion; in particular, with reference to Fig. 1 where we show schematically our physical model, if  $z(t) = -Z \cos \bar{\omega} t$  is the vertical sinusoidal time-history displacement applied to the support, the generic  $i$ -th pendulum of the chain is described by the following equation of motion, in terms of the angle  $\theta_i$  which defines its configuration:

$$mL^2 \ddot{\theta}_i + c \dot{\theta}_i + mgL \sin \theta_i + m\ddot{z}L \sin \theta_i + F_{i,i-1}L(\cos \alpha_{i,i-1} \cos \theta_i + \sin \alpha_{i,i-1} \sin \theta_i) + F_{i+1,i}L(\cos \alpha_{i+1,i} \cos \theta_i + \sin \alpha_{i+1,i} \sin \theta_i) = 0, \quad (1)$$

with

$$\begin{aligned}
\alpha_{i,i-1} &= \arctan\left(\frac{L\cos\theta_{i-1} - L\cos\theta_i}{H + L\sin\theta_i - L\sin\theta_{i-1}}\right), \\
d_{i,i-1} &= \sqrt{(H + L\sin\theta_i - L\sin\theta_{i-1})^2 + (L\cos\theta_{i-1} - L\cos\theta_i)^2}, \\
F_{i,i-1} &= K(d_{i,i-1} - H), \\
\alpha_{i+1,i} &= \arctan\left(\frac{L\cos\theta_i - L\cos\theta_{i+1}}{H + L\sin\theta_{i+1} - L\sin\theta_i}\right), \\
d_{i+1,i} &= \sqrt{(H + L\sin\theta_{i+1} - L\sin\theta_i)^2 + (L\cos\theta_{i+1} - L\cos\theta_i)^2}, \\
F_{i+1,i} &= K(d_{i+1,i} - H),
\end{aligned} \tag{2}$$

where  $i = 2, \dots, N-1$ , as the two edge pendula are subjected to only one elastic force of attraction/repulsion ( $F_{i+1,i}$  for the first pendulum and  $F_{i,i-1}$  for the last one).

In our notation  $\theta_i$  is the angular displacement of the  $i$ -th pendulum (positive rotation is anticlockwise and  $\theta_i = 0$  corresponds to the lowest position),  $m$  is the mass,  $c$  is the viscous damping coefficient,  $K$  is the coupling coefficient between each pair of pendula,  $L$  is the length of the pendula arm,  $H$  is the distance between the pivots of two adjacent pendula,  $g$  is the gravity acceleration; dots denote differentiation with respect to time.

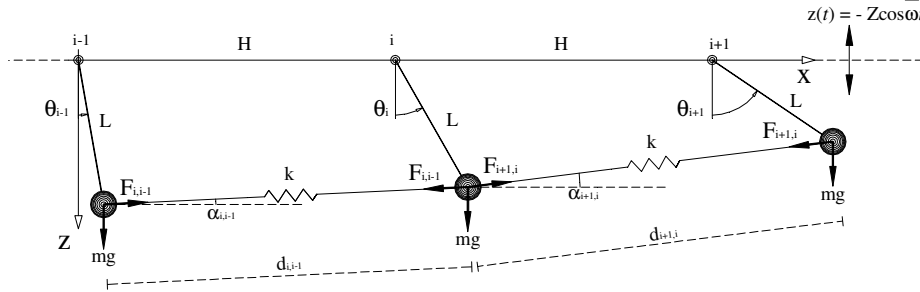


Figure 1: Physical model of the pendula chain with parametric vertical excitation: scheme of the forces acting on the  $i$ th generic intermediate pendulum.

The system of Eq. 1 can be rewritten in terms of the scaled dimensionless time  $\tau = \omega_p t$ , in order to obtain a form in which all variables and parameters are dimensionless:

$$\begin{aligned}
\ddot{\theta}_i + h\dot{\theta}_i + \sin\theta_i + A\cos(\omega\tau)\sin\theta_i + \frac{F_{i,i-1}}{mL\omega_p^2}(\cos\alpha_{i,i-1}\cos\theta_i + \sin\alpha_{i,i-1}\sin\theta_i) + \\
- \frac{F_{i+1,i}}{mL\omega_p^2}(\cos\alpha_{i+1,i}\cos\theta_i + \sin\alpha_{i+1,i}\sin\theta_i) = 0
\end{aligned} \tag{3}$$

with

$$\omega_p = \sqrt{\frac{g}{L}}, \quad h = \frac{c}{mL^2\omega_p}, \quad \kappa = \frac{K}{m\omega_p^2}, \quad \omega = \frac{\bar{\omega}}{\omega_p}, \quad A = \frac{Z}{L}\omega^2, \tag{4}$$

where  $h$  is the relative damping coefficient,  $\kappa$  is the coupling constant,  $\omega$  and  $A$  are the nondimensional frequency and amplitude of the vertical parametric excitation, respectively.

### 2.1 Dynamics of the chain and synchronization phenomena

In this work, numerical analysis techniques are employed to explore the dynamic responses to different parameters and initial conditions. Particularly, time histories, phase trajectories, the parameter space and bifurcation diagrams are used to explore the oscillatory, rotational and chaotic motions of the system.

We also draw some considerations about the synchronization and de-synchronization phenomena occurring between the pendulums of the chain, in relationship to the initial conditions assigned to the pendulums. The synchronization-desynchronization characteristics are evaluated both through the comparative analysis of the time histories of the single pendulums of the chain, and through the investigation of a correlation function:

$$C(jT) \equiv \frac{2}{N(N-1)} \sum_{(il)} \cos\langle \theta_i(jT) - \theta_l(jT) \rangle, \quad (5)$$

which expresses the global synchronization degree over all pairs of pendula. In Eq. (5)  $j$  is an integer multiple of the excitation period  $T \equiv 2\pi/\omega$ . We highlight that the function  $C$  assumes values in the range  $[-1, 1]$ , being 1 in the case of perfectly synchronized in phase pendula and -1 in the case of perfectly synchronized in counter-phase pendula; the desynchronized states live between these two extremes, with  $C(t)=0$  for the perfectly desynchronized state.

The nondimensional equations of motion, Eqs. (3), are numerically integrated using a fourth order Runge-Kutta algorithm with variable time step. The dynamics is therefore investigated by means of self-made codes within the Matlab environment and Fortran codes.

In our analyses we consider a chain of  $N = 5$  pendulums. The system motion depends on the initial conditions and on the system parameters. We assume, as reference case for our analyses, an initial system in which all the pendulums of the chain are parametrically excited in the vertical direction, without any other excitation (neither parametric, nor external). In this situation, we consider the same initial conditions for the motion of each pendulum (i.e. same rotation angle and same angular velocity): in particular we assume  $\theta_i=0$  and  $\dot{\theta}_i=1$ ; the coupling constant is assumed  $K = 1$  and the damping coefficient  $h = 0.1$ , while the other parameters of the pendulums, such as the mass and the length of the rod, are not of interest and are set equal 1, as we implement the equations of motion in nondimensional form. We perform simulations by varying the vertical excitation parameters, i.e. the nondimensional frequency  $\omega$  and amplitude  $A$ , in meaningful ranges of values: respectively in the ranges  $1 \div 2.6$  and  $0 \div 1.6$ ; in particular, the values of the excitation frequency have been chosen by considering only the major instability zone for the single parametric pendulum, which is around  $\omega = 2$  [1]. For each couple  $(\omega, A)$ , if we map the corresponding maximal Lyapunov exponent of the system, distinguishing its negative and positive values with different colors (respectively green and red), we observe a quite large zone of chaotic behaviour for values  $\omega$  and  $A$  in agreement with those obtained by Szemplinska-S. et al. [1] for the case of single pendulum with the same type of vertical parametric excitation (see our Fig. 2 in comparison with Fig. 4 in [1]). This means that, as expected,  $N$  pendulums, starting with the same initial conditions, behave as they were only one pendulum, i.e. they are perfectly synchronized. This result is confirmed by the values of the correlation function we obtain for each point in Fig. 2:  $C(t)=1$ .

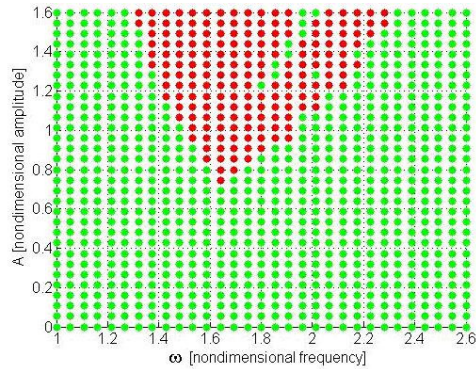


Figure 2: Grid of 30x30 points in the  $(\omega, A)$  parameter plane for the five pendula chain subjected to a chaos inducing vertical excitation; red (green) points denote that the respective maximal LE is positive (negative).

We highlight that the Lyapunov exponents of the system, used to create the map in Fig. 2, are computed using a version of the algorithm introduced in [22] and re-proposed and described in [23]; the integration is typically up to 10000 drive cycles for each fixed set of parameters.

The diagram in Fig. 2 covers the zone of existence and coexistence of the equilibrium attractor ( $\theta_i = \dot{\theta}_i = 0$ ), the  $2T$ -periodic oscillatory attractor, two  $T$ -periodic rotating attractors (anticlockwise and clockwise) and the steady-state tumbling chaos (TC). In order to put in evidence the possible various types of motion of the synchronized pendula, we focus on some couples of parameters  $(\omega, A)$  in Fig. 2 and we perform some numerical simulations by analyzing for each pendulum the time-histories of the rotation angle and of the angular velocity, and the phase plane diagram.

Firstly we assign the same initial conditions ( $\theta_i = 0$  and  $\dot{\theta}_i = 1$ ) to all the oscillators ( $N=5$ ); we test the point  $(\omega = 2, A=0.3)$ , and we obtain the  $2T$ -periodic oscillatory solution shown in the following Figs. 3, 4. We highlight that each of the  $N$  pendula exhibits the same behaviour, i.e. it is perfectly synchronized with the others, as it is also confirmed by the analysis of the relative correlation function  $C(t)$  (Fig. 3c). Therefore in Fig. 3 we report the time series of the rotation angle only for a sample of two pendula and in Fig. 4 the time series of the velocity and the phase plane diagram only for the first pendulum of the chain.

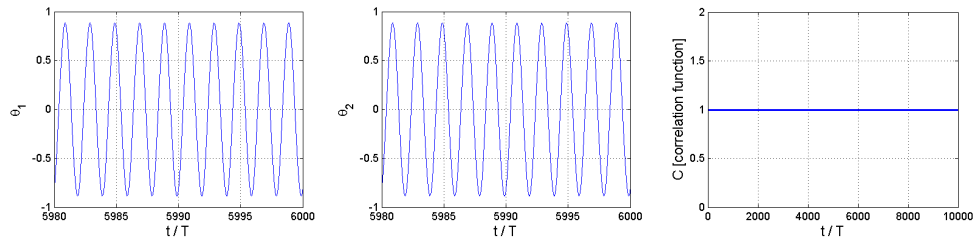


Figure 3: (a)-(b) Sample of the time history of the rotation angle vs. drive cycles ( $T \equiv 2\pi / \omega$ ) for a chain of five pendula, with same initial conditions and with excitation parameters  $\omega = 2, A=0.3$ ; the integration is up to 10000  $T$ ; (c) Correlation function  $C(t)$ .

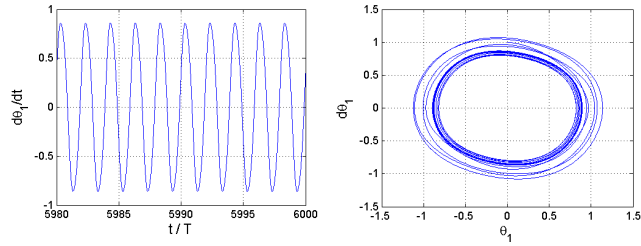


Figure 4: (a) Time series of the velocity and (b) phase plane diagram for the first pendulum.

If we change the initial conditions of the second pendulum ( $\theta_2 = \dot{\theta}_2 = 0$ ) and we leave the rest unchanged, we observe that after an initial transient the system tends towards the in-phase perfectly synchronous state of periodic oscillation (Fig. 5):  $C(t)$  approaches to unit.

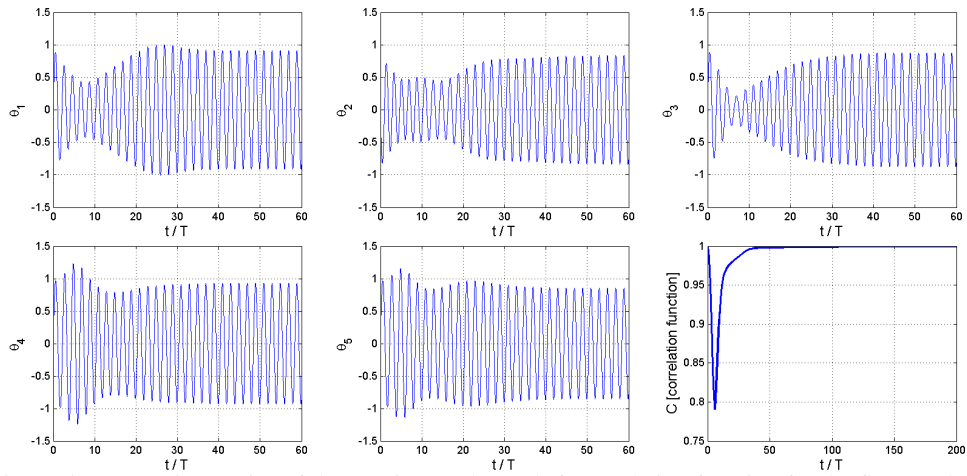


Figure 5: (a)-(e) Time series of the rotation angles and (f) correlation function for the five pendula with different initial conditions; excitation parameters:  $\omega = 2$ ,  $A=0.3$ .

For ( $\omega = 1.6$ ,  $A=0.3$ ), after a little transient we find the equilibrium attractor (hanging position,  $\theta_i = \dot{\theta}_i = 2n\pi$ ,  $n=0,1,2,\dots$ ); the tendency of the system towards the stable trivial solution is clearly shown, for the first pendulum, in the following Fig. 6 as well as the synchronized state of the chain expressed by the correlation function  $C(t)$ .

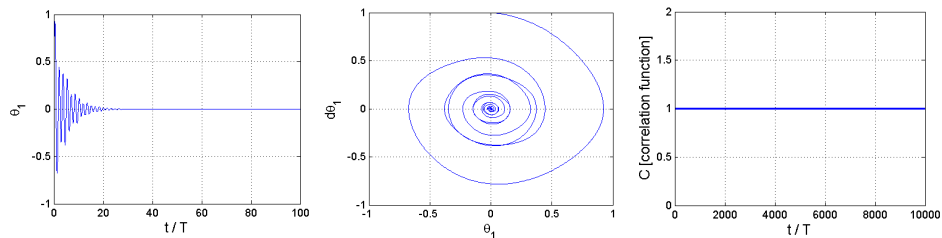


Figure 6: (a) Rotation angle and (b) phase plane diagram ( $\omega = 1.6$ ,  $A=0.3$ ); (c) correlation function.

By considering different points  $(\omega, A)$  inside the green region of Fig. 2 we can have also synchronous stable rotating clockwise or anticlockwise motions for the five pendula of the chain.

In the red region of Fig. 2 the steady-state tumbling chaos lives; for each couple of parameters inside this region, all the pendula of the chain exhibit the same tumbling chaos, provided that their motion starts with the same initial conditions. In Fig. 7 we show the result of a simulation performed for a parameters couple belonging to the lower bound of this region ( $\omega=1.6, A=0.87$ ); we consider the usual initial conditions  $\theta_i=0$  and  $\dot{\theta}_i=1, i=1, \dots, N$ .

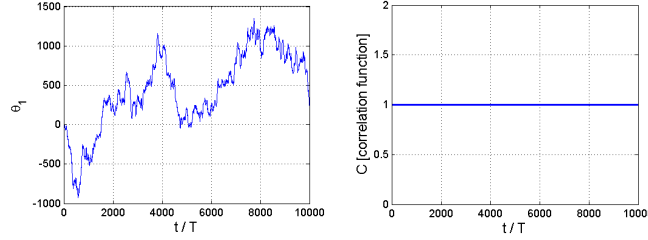


Figure 7: (a) Time history of the rotation angle vs. drive cycles for the first pendulum of the chain: the others follow exactly the same behaviour, starting with the same i.c.; excitation parameters  $\omega=1.6, A=0.87$ ; (b) Correlation function  $C(t)$ .

Here the pendula are perfectly synchronized ( $C(t)=1$ , Fig. 7b), but it is sufficient to change the initial conditions even for only one pendulum, for example the second ( $\theta_2=\dot{\theta}_2=0$ ), that we lose the synchronized state (Fig. 8c), and the TC time histories and orbits in the phase plane for the  $N$  pendula are no more coincident. Accordingly, the correlation function  $C$  fluctuates within its range of definition without never achieving the unitary value: no synchrony is possible.

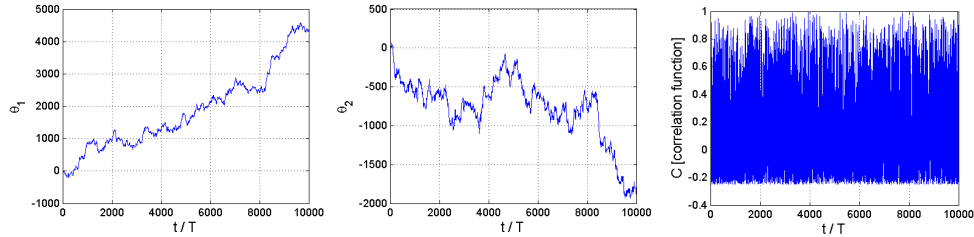


Figure 8: (a), (b) Time series of the rotation angle for the first two pendula, in case of different initial conditions between pendula; excitation parameters  $\omega=1.6, A=0.87$ ; (c) Correlation function.

We highlight that the system, and therefore its capability to achieve the synchronized state, is sensitive to the initial conditions assigned to the various oscillators of the chain.

### 3 CONTROL SCENARIO

We study and test the possibility to control the chaotic dynamics of the system by applying a horizontal excitation to the point of support of the two edge pendula of the chain; in Fig. 9 we show schematically our physical model, by highlighting the two different types of parametric excitation: the vertical one, inducing chaos (CI), and the horizontal one, intended to control chaos (CC).

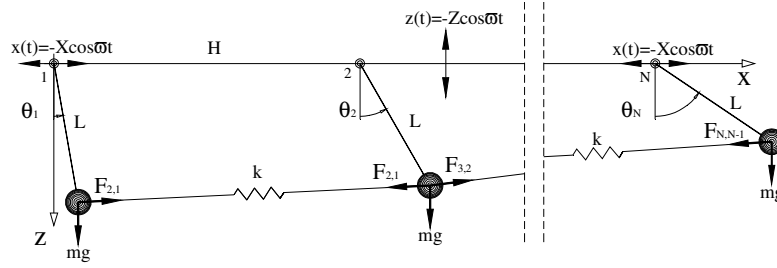


Figure 9: Control scenario: the CI vertical excitation is applied to all pendula, the CC horizontal one only to the first and to the last one.

Firstly, for the sake of concreteness, we study the application of such a control scenario to the paradigmatic example of only one dissipative Kapitza pendulum, described by the nondimensional equation:

$$\ddot{\theta} + h\dot{\theta} + \sin\theta + A\cos(\omega_{CI}t)\sin\theta + \varepsilon A\cos(\omega_{CC}t + \phi)\cos\theta = 0, \quad (6)$$

where  $\omega_{CI} = \omega$  and  $\omega_{CC}$  are, respectively, the nondimensional frequencies of the parametric vertical and horizontal excitation,  $\varepsilon A$  and  $\phi$  are the normalized amplitude and initial phase of the horizontal controlling excitation, while  $A$  is the normalized amplitude of the chaos inducing vertical excitation; therefore  $\varepsilon$  expresses the factor of the control amplitude with respect to the initially assigned parametric excitation amplitude.

In this work we analyze the case of main resonance between the two involved parametric excitations ( $\omega = \omega_{CI} = \omega_{CC}$  is their common frequency) and we try to study, from a numerical point of view, the possibilities to regularize the chaotic dynamics of the chain by varying the characteristics of the controlling excitation, in terms of initial phase difference ( $\phi$ ) and of amplitude ratio ( $\varepsilon$ ) with the chaos inducing vertical excitation. Hence we are now interested in exploring the  $\phi$ - $\varepsilon$  parameter plane.

Computer simulations of Eq. (6) have been performed by considering again the parameters values ( $m, L, h, K$ ) already used above and initial conditions  $\theta = 0$  and  $\dot{\theta} = 1$ . The nondimensional frequency and amplitude of the parametric vertical excitation ( $\omega, A$ ) are chosen inside the tumbling chaos (TC) region depicted in red in Fig. 2: we select a point belonging to the lower bound of this region ( $\omega = 1.6, A = 0.87$ ). Our numerical results are expressed in terms of negative/positive maximal Lyapunov exponent (LE) for each couple of values ( $\phi, \varepsilon$ ) in the parameter plane. LEs are computed once again using a version of the algorithm introduced in [22, 23] and the integration is typically up to 10000 drive cycles for the fixed parameters  $h, K, A, \omega$ . In the absence of the CC excitation ( $\varepsilon = 0$ ), the dissipative Kapitza pendulum exhibits a chaotic strange attractor characterized by a maximal LE  $\lambda^+(\varepsilon = 0) = 0.061$ . In the presence of the CC excitation, the maximal LE is calculated for each point on a 100x100 grid, with normalized initial phase  $\phi$  and amplitude ratio  $\varepsilon$  along the horizontal and vertical axes, respectively. The ranges of interest, we consider in our simulations, are  $0 \div 2\pi$  for  $\phi$  and  $0 \div 1.6$  for  $\varepsilon$ . The results are shown in the following Fig. 10. This diagram is constructed similarly to those of Fig. 2, by plotting in the ( $\phi, \varepsilon$ ) plane only red or green points when the respective maximal LE is positive or negative. Therefore the green points in Fig. 10 yield the characteristics ( $\phi, \varepsilon$ ) of the control excitation for which the homoclinic chaos is suppressed; the extension of the green area provides a simple quantifier of the



suppressive effectiveness of the CC excitation. From Fig. 10 we observe that complete regularization ( $\lambda^+(\varepsilon > 0) < 0$ ) mainly appears in certain regions which are periodically distributed along the  $\phi$ -axis, with fundamental period equal to  $\pi$ ; moreover the widest ranges of the suppressory phase difference are centred at the values  $\phi_{sup} = \{\pi/2, 3\pi/2\}$ , which therefore assume the meaning of optimal values. The maximum enhancement of chaos occurs at  $\phi_{enh} = \{0, \pi\}$ . We remark the double role enhancer/suppressor of the phase difference in the quite large range of relative amplitudes we have considered in our study.

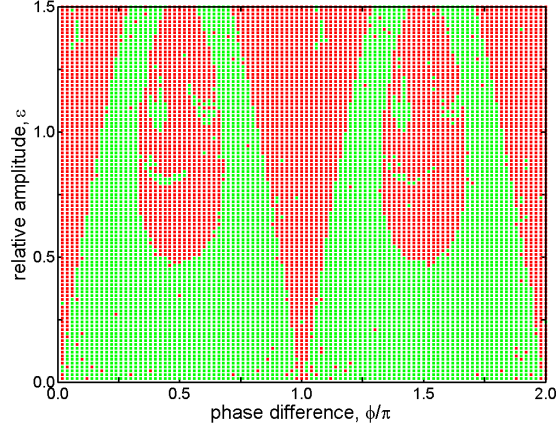


Figure 10: Maximal LE  $\lambda^+$  versus phase difference  $\phi$  and relative amplitude  $\varepsilon$  for a grid of 100x100 points in the parameter plane  $\phi - \varepsilon$ . Red and green squares indicate that the respective maximal LE is  $\lambda^+(\varepsilon > 0) \geq 0$  and  $\lambda^+(\varepsilon > 0) < 0$ , respectively.

Then we consider in the following the application of the above control scenario to the generic chain of  $N$  nonlinearly coupled pendula described by Eq. 3. The effectiveness of the control method under localized application of the CC excitations on a minimal number of pendula [24] (the first and the last of the chain, see Fig. 9) is studied again for the case of the main resonance between the two different kinds of involved parametric excitations (one chaos-inducing and the others chaos-controlling). Therefore the nondimensional equations of motion for the two edge pendulums with control become:

$$\begin{aligned}
\ddot{\theta}_1 + h\dot{\theta}_1 + \sin \theta_1 + A \cos(\omega_{C1}t) \sin \theta_1 + \varepsilon A \cos(\omega_{CC}t + \phi) \cos \theta_1 + \\
- \frac{F_{2,1}}{mL\omega_p^2} (\sin \alpha_{2,1} \sin \theta_1 + \cos \alpha_{2,1} \cos \theta_1) = 0, \\
\ddot{\theta}_5 + h\dot{\theta}_5 + \sin \theta_5 + A \cos(\omega_{C1}t) \sin \theta_5 + \varepsilon A \cos(\omega_{CC}t + \phi) \cos \theta_5 + \\
+ \frac{F_{5,4}}{mL\omega_p^2} (\sin \alpha_{5,4} \sin \theta_5 + \cos \alpha_{5,4} \cos \theta_5) = 0,
\end{aligned} \tag{7}$$

with the same meaning, already assumed in the previous case, for all variables and parameters.

Thus, with fixed values of  $h$ ,  $A$  and  $\omega$  corresponding to a given initial chaotic state of the synchronized pendula, there are only three independent parameters characterizing the control

scenario:  $\varepsilon$ ,  $\phi$  and  $\kappa$ (or  $K$ ).

We assume  $\omega=1.6$ ,  $A=0.87$  (TC) and we fix the coupling constant  $K=1$ . The same initial conditions for all the five pendulums are considered ( $\theta_i=0, \dot{\theta}_i=1$ ). In the absence of any control ( $\varepsilon=0$ ), the chain exhibits a strange chaotic attractor with a maximal LE  $\lambda^+(\varepsilon=0) = 0.10826$ ; in the following Fig. 11 we show the time series of this maximal LE.

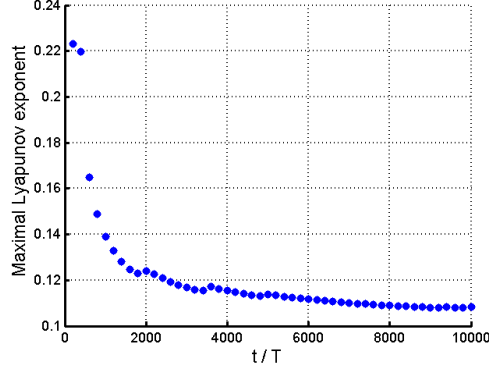


Figure 11: Maximal LE  $\lambda^+$  versus drive cycles for the chain of five pendula without any control excitation ( $\varepsilon = 0$ ). Parameters are:  $\omega=1.6$ ,  $A=0.87$ ,  $h=0.1$ ,  $K=1$ .

Lyapunov exponent (LE) calculations of the five pendula chain, subjected to the aforementioned type of chaos-controlling excitation (Eq. 7), are then performed by varying the control parameters  $\varepsilon$  and  $\phi$  in the same ranges we have considered for the pilot case of single pendulum.

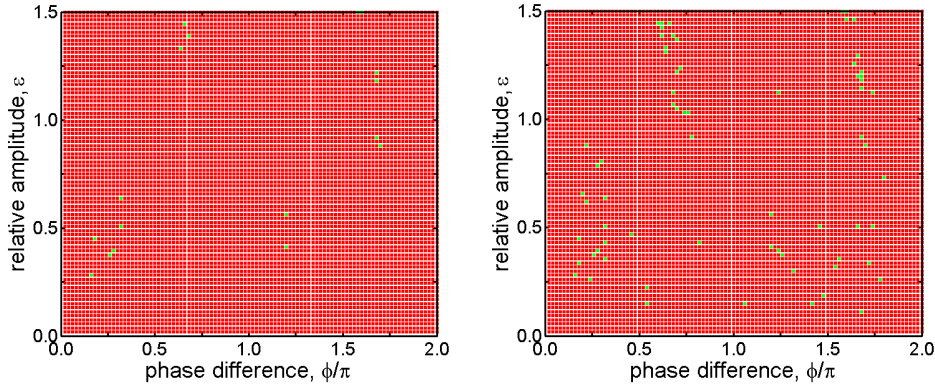


Figure 12: Maximal LE  $\lambda^+$  versus phase difference  $\phi$  and relative amplitude  $\varepsilon$  for a grid of 100x80 points in the parameter plane  $\phi - \varepsilon$ . Red and green squares indicate that the respective maximal LE is  $\lambda^+(\varepsilon > 0) \geq 0$  and  $\lambda^+(\varepsilon > 0) < 0$ , respectively. (a) First pendulum and (b) third pendulum.

By comparing Fig. 10 with Fig. 12, we observe that the numerical predictions obtained for the single pendulum and those obtained for the chain provide a completely different scenario in terms of wideness of the regularization areas. We also highlight that, while in the single pendulum case

(Fig. 10) the regularization areas are almost perfectly periodic along the  $\phi$ -axis with fundamental period equal to  $\pi$ , in the chain the numerically detected regularization points, when present, are distributed in an almost casual manner along the horizontal axis, even if for the central pendulum a sort of periodicity can be observed (see Fig. 12b).

In order to study both the effect of the localized controlling resonant forces and their capability to propagate from the edge pendulums thus affecting the dynamical behaviour of the central pendulum of the chain, we have actually monitored also this central pendulum (which is the third one in our case, see Fig. 12b). We observe that, for the parameters values we have considered, the localized controlling resonant forces-induced regularization is slightly more effective on the 3rd pendulum, where the effect of the horizontal driving forces is not direct but it is transmitted by the mutual coupling between adjacent pendulums. Therefore, in general, chaos is enhanced and not suppressed in the two edge pendulums of the chain when we apply the CC excitation, while the effect of regularization is observable as we move away from the ends towards the central pendulum.

Moreover, by analyzing the time-histories in a point of the diagram of Fig. 12, we can observe that, at least in the weak coupling regime we have considered here ( $K=1$ ), the control acts like a de-synchronizer for the chain (Fig. 13), i.e. its effects in terms of synchronization are similar to those we obtain in the uncontrolled chain in case of different initial conditions assigned to the pendula: the correlation function  $C(t)$  assumes a fluctuating trend within its range of definition, without achieving the unitary value (Fig. 13f).

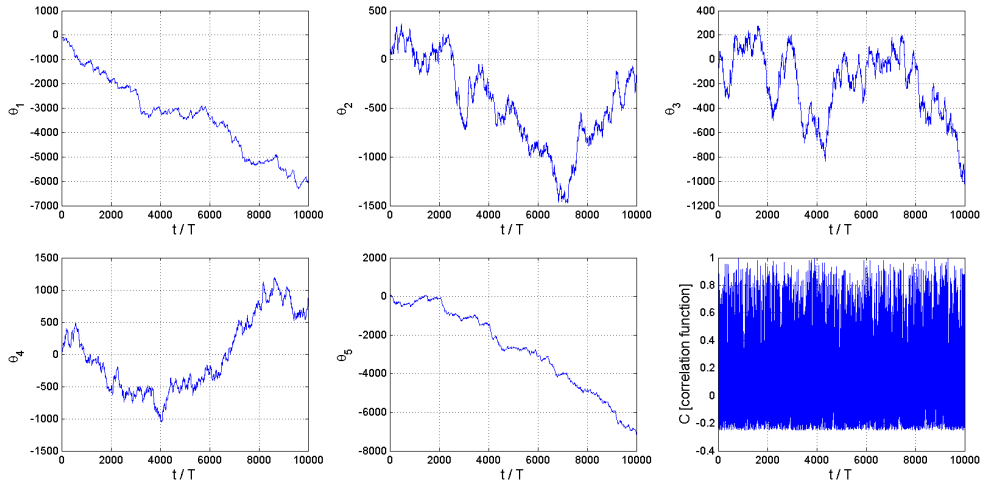


Figure 13: (a)-(e) Time histories of the rotation angle vs. drive cycles for our chain of five pendula, with same i.c., but with a CC horizontal excitation applied to the two edge pendula. Parameters:  $h=0.1$ ,  $K=1$ ,  $\omega=1.6$ ,  $A=0.87$ ,  $\phi=\pi/2$ ,  $\varepsilon=0.25$ . (f) Correlation function.

Finally we highlight that the pilot case of single pendulum with control, described by Eq. 6, is also equivalent to consider a chain with the two edge pendula characterized by a weak, almost inexistent coupling  $K$  with the adjacent pendulum.

#### 4 CONCLUSIONS

We have introduced the model of a chain of  $N$  identical chaotic parametric pendula, which are nonlinearly coupled between them. We have investigated the dynamics of this multidimensional system, with attention also to the possible synchronization/de-synchronization phenomena in the weak coupling regime. A correlation function between all pairs of pendula has been used in order to evaluate the degree of synchronization of the system. We have found that if all the pendula start their motion with the same initial conditions, they behave as they were only one, i.e. they are perfectly synchronized; under the periodic vertical parametric excitation, applied to the points of support of the pendula, this synchronized state keeps indefinitely unchanged, unless some other external factor occurs. We have pointed out the existence of a certain sensitivity of the synchronized steady-state of the system to the initial conditions assigned to the various pendula of the chain; in any case this sensitivity strongly depends on the degree of synchronization which characterizes the starting motion of the system (e.g. initial conditions equal or different for the pendula) and on the type of motion associated with the excitation parameters.

Through the paradigmatic example of a dissipative Kapitza pendulum, where chaos is induced by an analogous parametric vertical excitation, we have checked the localized application of a second parametric excitation on a minimal number of pendula in our chain, with the aim of controlling the chaotic dynamics. Numerical results show that the initial phase difference between the two excitations (chaos-inducing and chaos-controlling) plays a fundamental role in the control scenario. The analysis of these results (Lyapunov exponents) allows us to characterize the regularization routes in the control parameter plane.

We have highlighted the capability of the localized controlling resonant forces to propagate from the edge pendulums, thus affecting the dynamical behaviour of the central pendulum of the chain; obviously this depends on the coupling regime. We expect that the coupling coefficient influences the regularization scenario and we deserve this study to a forthcoming work: here we only guess that the efficiency of the localized horizontal excitation in regularizing the dynamics of the chain increases as the coupling increases, while the whole chain goes from a desynchronized state to a perfect synchronized state.

In view of the generality of the present control method, as well as its great flexibility and scope, our study can be seen as a first step to deduce a criterion which can be useful in choosing, in the  $(\phi, \varepsilon)$  parameter plane, the most suitable of the possible chaos-suppressing excitations, and, in the coupling constant range, the most suitable coupling constant  $K$  able to produce the perfect synchronization of the chain, even in case of different starting motions of the single pendula.

The authors wish to gratefully acknowledge the support of the Italian and Spanish Ministries of Higher Education and Research (MIUR and MEC, respectively) within the cooperation project "Integrated Action Italy-Spain" IT00777A9DL – HI2006-0157.

#### References

- [1] Szemplinska-Stupnicka, W., Tyrkiel, E. and Zubrzycki, A., "The global bifurcations that lead to transient tumbling chaos in a parametrically driven pendulum," *Int. J. Bifurcation and Chaos*, **10**, 2161-2175 (2000).
- [2] Pikovsky, A., Rosenblum, M.G. and Kurths, J., *Synchronization: a universal concept in nonlinear science*, Cambridge University Press, Cambridge, (2001).
- [3] Strogatz, S., *Sync: the emerging science of spontaneous order*, Hyperion, New York, (2003).
- [4] Uchida, A., Sato, T., Ogawa, T. and Kannari, F., "Nonfeedback control of chaos in a

- microchip solid-state laser by internal frequency resonance,” *Phys. Rev. E*, **58**, 7249-7255 (1998).
- [5] Ottino, J.M., Muzzio, F.J., Tjahjadi, M., Franjione, J.G., Jana, S.C. and Kusch, H.A., “Chaos, Symmetry, and Self-Similarity: Exploiting Order and Disorder in Mixing Processes,” *Science*, **257**, 754-760 (1992).
- [6] Andreyev, Y.V., Belsky, Y.L., Dmitriev, A.S. and Kuminov, D.A., “Information processing using dynamical chaos: Neural networks implementation,” *IEEE Trans. Neur. Networks*, **7**, 290-299 (1996).
- [7] Ding, W.X., She, H.Q., Huang, W. and Yu, C.X., “Controlling chaos in a discharge plasma,” *Phys. Rev. Lett.*, **72**, 96-99 (1994).
- [8] Schiff, S.J., Jerger, K., Duong, D.H., Chang, T., Spano, M.L. and Ditto, W.L., “Controlling chaos in the brain,” *Nature*, **370**, 615-620 (1994).
- [9] Gregoriou, G.G., Gotts, S.J., Zhou, H. and Desimone, R., “High-Frequency, Long-Range Coupling Between Prefrontal and Visual Cortex During Attention,” *Science*, **324**, 1207-1210 (2009).
- [10] Strogatz, S.H., Abrams, D.M., McRobie, F.A., Eckhardt, B. and Ott, E., “Crowd synchrony on the Millennium Bridge,” *Nature*, **438**, 43-44 (2005).
- [11] Lenci, S. and Marcheggiani, L., “A discrete-time model for the phenomenon of synchronous lateral excitation due to pedestrians motion on footbridges,” in *Proc. Third International Conference Footbridge 2008*, FEUP, Porto, Portugal, July 02-04, 2008.
- [12] Chacon, R., *Control of homoclinic chaos by weak periodic perturbations*, World Scientific Publishing, London, (2005).
- [13] Boccaletti, S., Grebogi, C., Lai, Y.C., Mancini, H. and Maza, D., “The control of chaos: theory and applications,” *Phys. Rep.*, **329**, 103-197 (2000).
- [14] Chen, G. and Dong, X., *From Chaos to Order*, World Scientific Publishing, Singapore (1998).
- [15] Ditto, W.L., Rauseo, S.N. and Spano, M.L., “Experimental control of chaos,” *Phys. Rev. Lett.*, **65**, 3211-3214 (1990).
- [16] Meucci, R., Gadomski, W., Ciofini, M. and Arecchi, F.T., “Experimental control of chaos by means of weak parametric perturbations,” *Phys. Rev. E*, **49**, R2528-R2531 (1994).
- [17] Boccaletti, S., *The Synchronized Dynamics of Complex Systems*, Elsevier, Amsterdam, (2008).
- [18] Dangoisse, D., Celet, J-C. and Glorieux, P., “Global investigation of the influence of the phase of subharmonic excitation of a driven system,” *Phys. Rev. E*, **56**, 1396-1406 (1997).
- [19] Schwartz, I.B., Triandaf, I., Meucci, R. and Carr, T.W., “Open-loop sustained chaos and control: A manifold approach,” *Phys. Rev. E*, **66**, 026213 (2002).
- [20] Chacón, R., “Melnikov method approach to control of homoclinic/heteroclinic chaos by weak harmonic excitations,” *Phil. Trans. R. Soc. A*, **364**, 2335-2351 (2006).
- [21] Guckenheimer, J. and Holmes, P.J., *Nonlinear Oscillations, Dynamical Systems, and Bifurcations of Vector Fields*, Springer, Berlin (1983).
- [22] Benettin, G., Galgani, L., Giorgilli, A. and Strelcyn, J.M., “Lyapunov characteristic exponents for smooth dynamical systems and for Hamiltonian systems; a method for computing all of them. Part 1: Theory. Part 2: Numerical Application,” *Meccanica*, **15**, 9-20, 21-30 (1980).
- [23] Wolf, A., Swift, J.B., Swinney, H.L. and Vastano, J.A., “Determining Lyapunov exponents from a time series,” *Physica D*, **16**, 285-317 (1985).
- [24] Chacon, R., Martinez, P.J., Martinez, J.A. and Lenci, S., “Chaos suppression and desynchronization phenomena in periodically coupled pendula subjected to localized heterogeneous forces,” *Chaos, Solitons & Fractals*, **42**, 2342-2350 (2009).